Proceedings of ICRC 2001: 2927 © Copernicus Gesellschaft 2001

ICRC 2001

Reconstruction of the EAS core position with the ARGO-YBJ detector

D. Martello [1], **C. Bleve**[1], **G. Di Sciascio**[2], **and the ARGO-YBJ Coll.**[*]

[1]Dip. di Fisica Universitá di Lecce e INFN sez. di Lecce, Lecce, Italy
[2]INFN sez. di Napoli, Napoli, Italy
[*]see ARGO-YBJ Coll. list

Abstract. The ARGO-YBJ detector is a full coverage array presently under construction at the Yangbajing Laboratory (Tibet, P.R. China, 4300 m a.s.l.). ARGO-YBJ will provide a detailed space-time picture of the front of small size air showers. In the analysis of the ARGO-YBJ data, a precise reconstruction of the shower parameters is of crucial importance to point to gamma ray sources. We present some different techniques exploited to determine the shower core position. The influence of the core reconstruction accuracy on the detector acceptance is discussed.

1 Introduction

The ARGO-YBJ detector is a full coverage array consisting of a single layer of RPCs with dimensions of $74 \times 78\ m^2$ (ARGO-YBJ Coll. (1996)). The area surrounding the central detector core, up to $\sim 100 \times 100\ m^2$, in partially ($\sim 50\%$) instrumented with RPCs. This outer guard-ring improves the apparatus performance, enlarging the fiducial area for the detection of showers with the core outside the central full coverage carpet.

The basic element providing the time pattern of the shower is the logical *pad*. It is defined as the fast-OR of 8 strips each $6\ cm$ wide and $62\ cm$ long used to pick up the signals of the RPC (C. Bacci et al. (2000)). These logical pads ($56 \times 62\ cm^2$) define the time and space granularity of the detector.

Usually, the algorithms to reconstruct the shower features are applied to the so-called *'Internal Events'*. In effect, rejecting *'External Events'* is beneficial as both angular resolution and background discrimination capability are worse for events with core out of the detector. As a consequence, the determination of the shower core position is the first step for further analysis. This goal can be achieved using different algorithms, the important quality factors to classify the various procedures being the *'efficiency'* (i.e., the percentage of the true internal events reconstructed as internal) and the *'contamination'* (i.e., the fraction of the true external events reconstructed erroneously as internal).

The problem of reconstructing the core position for a single event is quite involved particularly for low multiplicity showers (i.e. showers with a low number of total fired pads) because of the large fluctuations which could make the actual shower image very different from the expected average one.

Some algorithms have been implemented and some preliminary results of their application are presented.

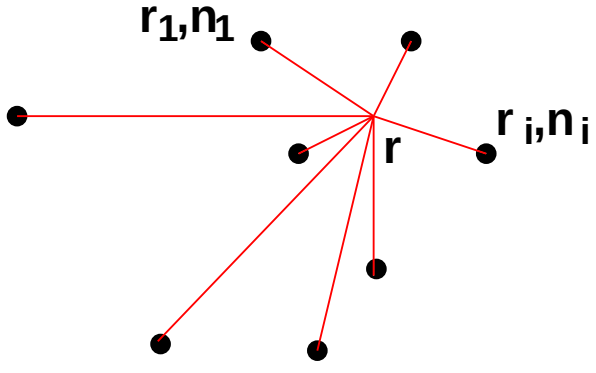

Fig. 1. Example of an **r**-tree.

2 Core reconstruction algorithms

2.1 Notation.

In the following paragraphs we use the symbols listed below:

N $\equiv$ pad multiplicity of a given event.

For the fired pad i ($i = 1, \cdots, N$):

x_i, y_i $\equiv$ pad centre coordinates on the detector plane

z_i $\equiv$ $t_i \cdot c_{light}$

t_i $\equiv$ pad time referred to the trigger time

n_i $\equiv$ number of fired strips

Correspondence to: D.Martello (martello@le.infn.it)

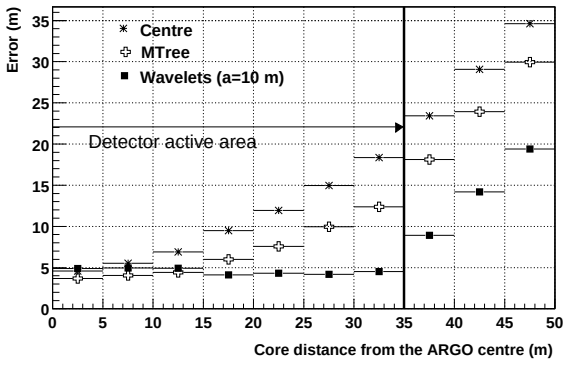

Fig. 2. Average error in core reconstruction as a function of the distance between the shower core position and the geometrical detector centre along the y axis.

The subscript **c** denotes the reconstructed core coordinates.

2.2 Centre of mass (`Centre`)

This method consists in calculating the average of the fired pad coordinates weighted by the number of fired strips:

$$(x_c, y_c) = \frac{\sum_{i=1}^{N} (x_i, y_i)\, n_i}{\sum_{i=1}^{N} n_i} \tag{1}$$

Due to its nature, the centre of mass algorithm tends to move the reconstructed core towards the detector centre. This introduces a systematic error dependent on the true position of the core.

2.3 Tree algorithm (`Tree`)

Given a set of points $\{\mathbf{P}(\mathbf{r_i})\}$, each one with an associated weight n_i, we call **r-tree** the set of lines joining a generic point $\mathbf{P}(\mathbf{r})$ with each of the $\mathbf{P}(\mathbf{r_i})$ (see fig. 1).

We can define the **r-tree length l(r)** as follows:

$$\mathbf{l}(\mathbf{r}) = \sum_{i=1}^{N} d(\mathbf{r}, \mathbf{r_i})\, n_i \tag{2}$$

where $d(\mathbf{r}, \mathbf{r_i})$ is the distance between **P(r)** and $\mathbf{P}(\mathbf{r_i})$.

This algorithm calculates, as a function of $\mathbf{r}$, the three dimensional tree length. The reconstructed core position is given by the x and y coordinates of the point $\mathbf{P}(\mathbf{r})$ whose tree length is minimal.

The basic idea is that a point which is in a cluster of hits has a tree lenght smaller than that of an isolated point.

2.4 Smoothing algorithm (`Wavelet`)

A simple idea to recover local fluctuations in the hit distribution consists in deriving a smoothed distribution f, which is the convolution of the experimental 2-dimensional density distribution with a properly chosen smoothing function g. The method first calculates $f(\mathbf{r_0})$ for each pad centre $\mathbf{r_0}$, whether the pad is fired or not, then it finds the absolute maximum of f: the corresponding value $\mathbf{r_0}$ is the reconstructed core position.

The function f calculated with this algorithm is the wavelet transform of the density distribution (I. Daubechies (1992)). We define

$$f(\mathbf{r_0}) = \int \rho(\mathbf{r}) \cdot g^{a,\mathbf{r_0}}(\mathbf{r})\, dV \tag{3}$$

where $\rho(\mathbf{r})$ is the density distribution, $g^{a,\mathbf{r_0}}(\mathbf{r}) = g(|\mathbf{r} - \mathbf{r_0}|/a)$ is called the mother wavelet and a is a scale parameter.

A standard choice for the mother wavelet is the so called *mexican hat function*:

$$g^{a,\mathbf{r_0}}(t) = (D - t^2)\, e^{-t^2/2} \tag{4}$$

where $t = \sqrt{\sum_{j=1}^{D}((x_j - x_0)/a)^2}$ is the euclidean distance (in a units) and D is the dimension of the space in which the density distribution $\rho(\mathbf{r})$ is defined.

Since we work in 2 dimensions (D=2) and since we deal with a discrete and finite distribution the calculated f is simply

$$f(\mathbf{r_0}) = \sum_{i=1}^{N} n_i\, (2 - t_i^2)\, e^{-t_i^2/2} \tag{5}$$

where t_i is the euclidean distance in a units between the i-th fired pad and $\mathbf{r_0}$. This function favours clusters of hits with relative distance of the order of a.

2.5 Maximum Likelihood Method (`LLF`)

If $< m_i >$ is the average particle number expected on the i-th pad, then the probability of finding N_i particles is

$$P_i = \frac{< m_i >^{N_i}}{N_i!} \cdot e^{-<m_i>}$$

Therefore $P_i(0) = e^{-<m_i>}$ is the probability of finding 0 particles, and $P_i(>0) = 1 - e^{-<m_i>}$ is the probability of finding 1 or more particles. The Likelihood Function (LF) is given by: $LF = \Pi_i P_i$. The natural Logarithm of LF (`LLF`) becomes a sum:

$$LLF = ln(\Pi_i P_i) = \Sigma_i ln P_i(0) + \Sigma_j ln P_j(>0)$$

where the index i runs on the not fired pads, while the index j refers to the fired pads. Therefore, we obtain

$$-LLF \equiv S_{pad} \cdot \Sigma_i \rho_i - \Sigma_j ln(\rho_j) - N_{pad}(>0) \cdot ln(S_{pad})$$

where $\rho_i = f(R_i/R_M) \cdot \frac{N_e}{R_M^2}$ is the particle density expected on the i-th pad at a distance R_i from the core, $f(R_i/R_M)$ is a lateral structure function NKG-like and R_M is the Moliere radius (133 m at the YBJ level). S_{pad} is the pad area and $N_{pad}(>0)$ is the total number of pads fired by the shower. The minimum value of (-LLF) is then chosen as the best fit for the freely varying parameters $\{x_c, y_c, N_e\}$, being $\{x_c, y_c\}$ the core coordinates and N_e the shower size.

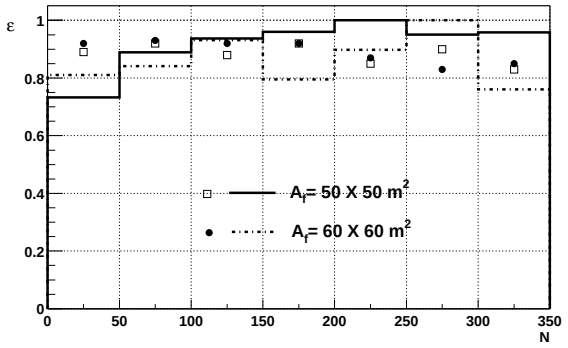

Fig. 3. Efficiency to identify *'internal'* events as a function of the pad multiplicity obtained with the `Wavelet` method (lines) and with the `LLF` method (markers)

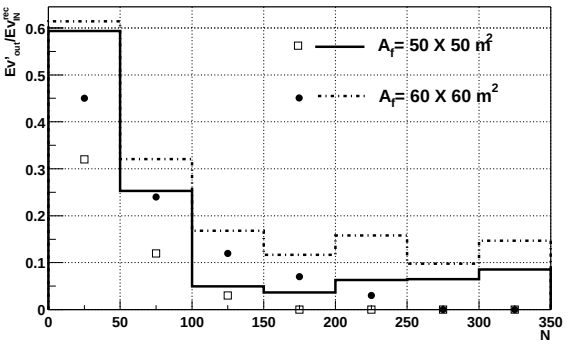

Fig. 4. Contamination of showers with core outside the fiducial area A_f as a function of the pad multiplicity. Lines and markers show the results obtained with the `Wavelet` and the `LLF` methods, respectively.

3 Results

The algorithms described in the previous section have been used to analyse 10^6 γ-initiated showers. To simulate the development of the EAS the Corsika 5.624 (D. Heck et al. (1998)) code has been used. The events have been generated with a uniform core distribution over an area $A = 500 \times 500\ m^2$ centred on the detector, with a zenith angle in the range $0-35^o$ and with a CRAB-like energy spectrum ($0.1 \rightarrow 10\ TeV$).

In fig.2 the dependence of the error on the core distance from the detector geometrical centre is shown. Clear systematic effects can be seen not only for `Centre` but also for `Tree`, while `Wavelet` reconstruction seems to be independent of the core position (when the core is inside the detector). Since all the algorithms reconstruct the core inside the apparatus, an increase in the reconstruction error can be seen in the case of external events.

While `Centre` and `Tree` reconstruct both internal and external showers with a core inside an area smaller than the carpet surface and inside the detector, `Wavelet` and `LLF` reconstruct the core position of external events near the edge of the detector. This fact suggests of defining a suitable fiducial area A_f smaller than the geometrical one in order to reject the external events.

The showers classified as *'internal'* events, that is showers (Ev^{rec}_{IN}) with the core reconstructed inside the fiducial area, include both true internal showers (Ev^{true}_{IN}), identified with efficiency ϵ, as well as a fraction of misreconstructed showers with core outside (Ev'_{OUT})

$$Ev^{rec}_{IN} = Ev^{true}_{IN} \cdot \epsilon + Ev'_{OUT}$$

Fig. 4 and Fig. 3 show the efficiency ϵ and the contamination Ev'_{OUT}/Ev^{rec}_{IN}, respectively, as a function of the pad multiplicity for two different fiducial areas $A_f = 50 \times 50\ m^2$ and $60 \times 60\ m^2$.

The core position resolution for the reconstructed internal events, calculated using the `Wavelet` and the `LLF` methods, is shown in Fig. 5 for different fiducial areas.

The core position resolution determined with the `LLF` method for low multiplicity seems more sensitive to the choice of the fiducial area than the `Wavelet` method. This is due to the larger contamination affecting the `Wavelet` method, being, for low multiplicity events, larger than 50%.

In fact, the poor resolution for low multiplicity events is largely dominated by the contamination from misreconstructed external showers.

4 Conclusions

Different methods have been implemented and used to analyse γ-initiated showers, the `Wavelet` and `LLF` seen the more promising ones.

While `Centre` and `Tree` reconstruct both internal and external showers with a core inside an area smaller of the detector area, `Wavelet` and `LLF` behaviour approaches the ideal one giving a distribution almost uniform for internal showers and peaked near the border for the external ones. This behaviour can be used to reject external showers with good efficiency.

The main advantage of these core reconstruction methods is that they are topological and don't need a precise reconstruction of the shower front, therefore they are indipendent from the angular resolution of detector.

The study of other methods to discriminate between internal and external events is in progress. These methods will take into account not only the topology of the detected shower but also the time features of the shower front. In fact, the ARGO-YBJ detector, due to its high granularity and excellent time resolution ($\sim 1\ ns$), will provide a highly detailed picture of the space-time pattern of the shower profile.

An improvement of the rejection power for the external events could be achieved taking into account the information provided by the *guard-ring* that will be deployed around the carpet to extend the fiducial area (ARGO-YBJ Coll. (1996)) (in this analysis the guard-ring has not be used). This will improve both the energy and the angular resolution of the

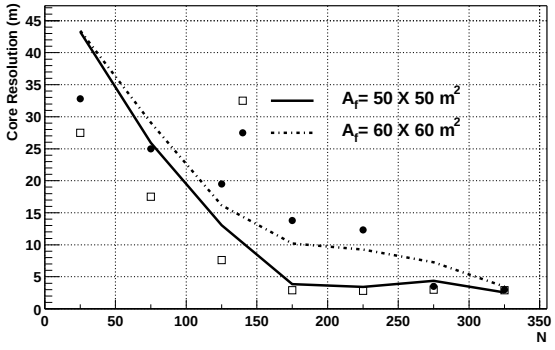

Fig. 5. Core position resolution as a function of the pad multiplicity. (Lines refer to `Wavelet` method while markers refer to `LLF`)

ARGO-YBJ detector and increase its hadronic cosmic ray rejection, thus improving its overall gamma-ray sensitivity.

References

ARGO-YBJ Coll., *Astroparticle Physics with ARGO*, Proposal ,1996. C. Bacci et al., *The ARGO-YBJ Project*, Addendum to the Proposal ,1998. These unpublished documents can be downloaded at the URL: http://www1.na.infn.it/wsubnucl/cosm/argo/argo.html

C. Bacci et al. (ARGO-YBJ Coll.), NIM **A443** (2000) 342.

I. Daubechies, *Ten Lectures on Wavelet* SIAM, Philadelphia (1992)

D. Heck, J. Knapp, J.N. Capdevielle, G. Schatz, and T. Thouw, Report **FZKA 6019** (1998), Forschungszentrum Karlsruhe